Study of nonlinear Poisson–Boltzmann equation for a rodlike macromolecule using the pseudo-spectral method

Article *in* Results in Physics · October 2017

DOI: 10.1016/j.rinp.2017.10.024

3 authors, including:

Houshyar Noshad
Amirkabir University of Technology
32 PUBLICATIONS **64** CITATIONS
SEE PROFILE

Esmaeil Motevali
Amirkabir University of Technology
2 PUBLICATIONS **0** CITATIONS
SEE PROFILE

Results in Physics 7 (2017) 3938–3945

Contents lists available at ScienceDirect

Results in Physics

journal homepage: www.journals.elsevier.com/results-in-physics

Study of nonlinear Poisson-Boltzmann equation for a rodlike macromolecule using the pseudo-spectral method

Shaghayegh Nikzad, Houshyar Noshad *, Esmaeil Motevali

Department of Energy Engineering and Physics, Amirkabir University of Technology (Tehran Polytechnic), Hafez Avenue, Tehran, Iran

ARTICLE INFO

Article history:
Received 25 July 2017
Received in revised form 9 October 2017
Accepted 9 October 2017
Available online 14 October 2017

Keywords:
Poisson-Boltzmann equation
Electric field
Pseudo-spectral method
Chebyshev functions
Legendre polynomials

ABSTRACT

The pseudo-spectral method with the Chebyshev and Legendre polynomials are used in order to compute the electric potential for a rodlike macromolecule located in salt free solution via the Poisson-Boltzmann equation (PBE). Afterwards, verification of the method is demonstrated for a long macromolecule as well as a large plate for which the behaviors can be properly explained by a one-dimensional PBE. It is concluded that the method based upon the Chebyshev polynomials with the specified collocation points is more accurate than the technique based on the Legendre polynomials with the same number of points. As a macromolecule has a rodlike shape, a two-dimensional PBE is considered, which corresponds to a much more realistic case. To solve the PBE, the concentration of the macromolecule in the solution and the electric field are used to compute the height and radius of the unit cell, which are obtained to be as 16.7 and 8.1 nm, respectively. It is worth noting that numerical computation of the PBE for a macromolecule with a finite length has not been reported previously using the pseudo-spectral method. The results given in this work can be appropriately used for stiff fragments of DNA and actin filaments.

Introduction

Electric charges and electrostatic interactions are ubiquitous in soft matter and biological systems [1,2] such as muscle, membrane, and protoplasm [3,4]. Soft materials are typically composed of macromolecules such as polymers, colloids and proteins, which often acquire surface charges when dissolved in a polar solvent like water. In recent years, the clustering of small ions around large, highly charged polyelectrolytes has been a major subject of interest in the field of electrolytes and polymers. Furthermore, the charged materials are considered as appropriate candidates for many technological applications, and on the other hand, a challenging subject for fundamental research in interdisciplinary sciences [5]. Moreover, the PBE has been used for electrostatic interactions between biological molecules in the saline and salt free solutions, which gives adequate description regarding the steady state electrostatic solution [6–8].

To solve this partial differential equation (PDE), the finite element method (FEM) has the limitations such as various instabilities in solution. To remove this difficulty, it is usually attempted to solve the PDE using smaller elements. This makes that the solution be difficult and in some cases impossible by the personal computers. In order to remove this limitation, some contributions in this field have been done using the meshless approaches [9] such as spectral element method (SEM), finite difference method [10], alternating-direction Sinc-Galerkin method (ADSG) [11], quadratic spline collocation method (QSCM) [12], Liu and Lin method [13]. It is notable that, the orthogonal functions and polynomials are employed in the SEM in order to transform the PDE into a set of equations [14–18]. This can be carried out by truncation of the series as well as the collocation method [19,20].

In this work, the PBE is solved for a finite rodlike macromolecule in salt free solution via the pseudo-spectral method. Some examples for such macromolecules are stiff fragments of DNA or actin filaments [21]. It is worth mentioning that numerical solution of the PBE for a macromolecule with a finite length has not been reported in the literature previously using this approach. The basic idea of all numerical techniques is to approximate any function by polynomials. Various types of numerical methods can be generated depending on the choice of trial functions or polynomials. In this paper, we are interested in spectral methods so that the global polynomials are the Legendre or the Chebyshev functions. The pseudo-spectral approach interpolates the solution of the differential equation with high accuracy based on least squares method [22–24]. It is notable that in our previous article [25], the FEM was used with the limitation which has been recently mentioned.

* Corresponding author.
E-mail address: hnoshad@aut.ac.ir (H. Noshad).

https://doi.org/10.1016/j.rinp.2017.10.024
2211-3797/

Whereas, spectral techniques are basically more evolved in comparison with finite difference schemes, because they allow us to obtain satisfactory accuracy with merely moderate computational resources. Moreover, in our previous work [25] the dimensions of the unit cell were considered using the concentration of counter ions [26,27]. Whereas, in the present study the dimensions of the unit cell are computed by taking into account the concentration of the macromolecule as well as computation of the corresponding electric fields using the Coulomb's law.

The article is organized as follows. The mathematical formalism and model are given in "Mathematical description and model". The numerical results are presented in "Numerical results and discussion". Finally, the paper is ended by a conclusion in "Conclusion".

Mathematical description and model

A two-dimensional nonlinear PBE in salt free solution has the following form.

$$\nabla^2 y(r,z) = \frac{K^2}{2}\exp(y(r,z)), \tag{1}$$

where the dimensionless parameter $y = e\Phi/k_BT$ is the reduced potential, and $K^2 = 8\pi l_B n$ denotes the screening potential in which $l_B = e^2/4\pi\varepsilon k_BT$ is defined as the Bjerrum length. In the relation, k_B and T stand for the Boltzmann constant and the temperature of the solution, respectively. The z axis is selected as the common axis of the charged macromolecule and the unit cell. The inside of the unit cell is electrically charged with the same electric charge in magnitude and opposite to that of the macromolecule, the so-called the counter-ions. Thus, it guarantees that the unit cell is electrically neutral. One can find from the literature [26] that the radius of the unit cell is reported as follows:

$$R_0 = \sqrt{\frac{1}{\pi bc}}, \tag{2}$$

where b and c are the distance between the two ionic groups and the concentration of the counter ions, respectively. It should be noted that the volume charge density of the counter-ions is not constant; instead it follows the Boltzmann distribution, and consequently Eq. (2) for R_0 cannot be correct. The following process demonstrates the exact values of the unit cell dimensions via our reasonable analysis.

The volume of each unit cell can be properly obtained via the following formula

$$\upsilon = \frac{V}{N} = \frac{1}{C}, \tag{3}$$

where

$$\upsilon = L\pi R^2. \tag{4}$$

In the relation (3), the quantities υ, C, N and V are the volume of the unit cell, the concentration of the macromolecule, the number of the macromolecules in the solution and the volume of the solution, respectively. Moreover, R and L stand for the radius as well as the height of the unit cell. Afterwards, the electric field of the macromolecule with surface charge density is computed using the Coulomb's law. As a consequence, the mean electric field is given as

$$\bar{E}_r = \frac{\int_{-l/2}^{l/2} E_r(r=a,\varphi=0,z)dz}{l}, \tag{5}$$

$$\bar{E}_z = \frac{\int_0^a E_z(r,\varphi=0,z=\pm\frac{l}{2})dr}{a}. \tag{6}$$

By using Eqs. (5) and (6) the ratio of ion concentrations around the macromolecule is specified. It should be noted that the electric field in each direction is proportional to the ion concentration and the dimensions of the unit cell. Hence, the definition mentioned below is valid

$$\frac{\bar{E}_r}{\bar{E}_z} = \frac{R-a}{\frac{L}{2}-\frac{l}{2}}. \tag{7}$$

Moreover, the volume of the unit cell is obtained by using the macromolecule concentration, which is calculated from Eq. (3). Eqs. (7) and (4) result in a set of nonlinear equations, which can be properly solved. Thus, for the macromolecule with the radius a = 0.5 nm and height l = 12 nm and also by considering the concentration of the macromolecule as $C = 4.8\times10^{-4}$M [27], the quantities R as well as L are obtained to be equal to 8.1 nm and 16.7 nm, respectively.

Afterwards, analytical derivations for the two extreme cases are presented as follows in order to show the validity of our approach. The first case is related to a one-dimensional PBE, which corresponds to a long macromolecule having a radius of 0.5 nm [27] in a salt free solution. The biological equivalent is indicated as the tobacco mosaic virus, which is a rodlike polyelectrolyte, and consequently, the results can be applied to study its behavior [26]. The one-dimensional PBE for the salt free solution has the following form [28]:

$$\left(\frac{d^2}{dr^2}+\frac{1}{r}\frac{d}{dr}\right)y(r) = \frac{K^2}{2}\exp(y(r)), \tag{8}$$

where the following boundary conditions should be satisfied

$$\left(\frac{dy}{dr}\right)_{r=R} = 0, \qquad \left(\frac{dy}{dr}\right)_{r=a} = -\frac{2\xi}{a}, \tag{9}$$

In the relation, the quantity ξ, the so-called the Manning parameter is equal to:

$$\xi = \frac{l_B}{b}. \tag{10}$$

One can find from the literature that the exact solution of Eq. (8) has the following form [26,28–30]:

$$y(r) = \ln\left[\frac{2\beta}{Kr\cos(\beta\ln\frac{r}{R_M})}\right]^2. \tag{11}$$

By substituting Eq. (11) into the boundary conditions (9), the constants β and R_M are computed to be 0.8 and 2.6 nm, respectively.

The second case, which also shows the validation of our analysis, is related to a one-dimensional PBE corresponding to a large plate for the salt free solution. The governing equation for the mathematical behavior of the system is given below

$$\frac{d^2}{dz^2}y(z) = \frac{K^2}{2}\exp(y). \tag{12}$$

The appropriate boundary conditions for the aforementioned equation are as follows

$$\left(\frac{dy}{dz}\right)_{z=l} = 0, \qquad \left(\frac{dy}{dz}\right)_{z=0} = -\frac{2\xi}{a}. \tag{13}$$

The boundary conditions are applied for the surface of the plate which is defined by z = 0, as well as the height $z = l$ for which the electric charge in the region $0 < z < l$ is considered to be equal to that of the plate, namely z = 0. By multiplying Eq. (12) with dy/dz, and hence, integrating with respect to z in the interval [l, z] as well as use of the boundary condition $(dy/dz)_{z=l} = 0$, one can obtain

$$\left(\frac{dy}{dz}\right)^2 = K^2\left(e^y - e^{y(l)}\right). \tag{14}$$

By integrating Eq. (14) over the same interval and performing some algebraic manipulations, the relation below may be obtained

$$y(z) = \ln\left[\exp(y_l)\sec^2\left(\frac{-\sqrt{\exp(y_l)}K(z-l)}{2}\right)\right], \tag{15}$$

where y_l means the value of y for a given l. Substituting Eq. (15) into the boundary condition $\left(\frac{dy}{dz}\right)_{z=0} = -\frac{2\xi}{a}$ yields

$$\tan\left(\frac{\sqrt{\exp(y_l)}lK}{2}\right) - \frac{2\xi\sqrt{\exp(y_l)}}{aK} = 0. \tag{16}$$

By solving Eq. (16), the value of y_l may be computed. The aforementioned analytical formulas, namely Eqs. (11) and (15), will be used in the next section in order to demonstrate the reliability of our approach.

In this article, the main objective is to solve the two-dimensional PBE based on the pseudo-spectral method. First, the mathematical formulation for a one-dimensional equation is discussed, and afterwards the stages for solving the two-dimensional PBE are presented.

Discretization of the PBE via the pseudo-spectral method

As stated above, this method interpolates the solution of the differential equations based on the least squares approximation. Therefore, the solution of the differential equation is properly approximated as follows.

$$y(r) \simeq u(\bar{r}) = \sum_{n=0}^{N} a_n \phi_n(\bar{r}), \tag{17}$$

where a_n for $n = 0,\ldots, N$ are the coefficients should be specified. Whereas, $\phi_n(\bar{r})$ is the orthogonal function, which can be considered as the Legendre polynomials or Chebyshev functions with the argument $\bar{r}$ in the interval $[-1, 1]$. Hence, the relation below is able to reproduce the corresponding interval for r, namely $[a, R]$,

$$r = \frac{1}{2}[(R-a)\bar{r} + a + R], \tag{18}$$

where

$$\frac{d}{dr} = \frac{2}{R-a}\frac{d}{d\bar{r}}. \tag{19}$$

Substituting Eqs. (17)–(19) into Eq. (8) gives the following set of nonlinear equations

$$\left(\frac{2}{(R-a)}\right)^2 \sum_{n=0}^{N} a_n \left.\frac{d^2\phi_n}{d\bar{r}^2}\right|_{\bar{r}=\bar{r}_i} + \frac{2}{[(R-a)\bar{r}_i + a + R]}\frac{2}{(R-a)}\sum_{n=0}^{N} a_n \left.\frac{d\phi_n}{d\bar{r}}\right|_{\bar{r}=\bar{r}_i} = \tag{20}$$

$$\frac{K^2}{2}\exp\left(\sum_{n=0}^{N} a_n \phi_n(\bar{r}_i)\right), \qquad i = 1,\ldots,N-1$$

with the boundary conditions below

$$\frac{2}{(R-a)}\sum_{n=0}^{N} a_n \left.\frac{d\phi_n}{d\bar{r}}\right|_{\bar{r}=1} = 0 \tag{21}$$

$$\frac{2}{(R-a)}\sum_{n=0}^{N} a_n \left.\frac{d\phi_n}{d\bar{r}}\right|_{\bar{r}=-1} = -\frac{2\xi}{a}. \tag{22}$$

Eqs. (20)–(22) form a set of nonlinear equations as follows.

$$\begin{cases} \frac{2}{(R-a)}\sum_{n=0}^{N} a_n \left.\frac{d\phi_n}{d\bar{r}}\right|_{\bar{r}=-1} = -\frac{2\xi}{a} \\ \left(\frac{2}{(R-a)}\right)^2 \sum_{n=0}^{N} a_n \left.\frac{d^2\phi_n}{d\bar{r}^2}\right|_{\bar{r}=\bar{r}_1} + \frac{2}{[(R-a)\bar{r}_1 + a + R]}\frac{2}{(R-a)}\sum_{n=0}^{N} a_n \left.\frac{d\phi_n}{d\bar{r}}\right|_{\bar{r}=\bar{r}_1} \\ = \frac{K^2}{2}\exp\left(\sum_{n=0}^{N} a_n \phi_n(\bar{r}_1)\right) \\ \left(\frac{2}{(R-a)}\right)^2 \sum_{n=0}^{N} a_n \left.\frac{d^2\phi_n}{d\bar{r}^2}\right|_{\bar{r}=\bar{r}_i} + \frac{2}{[(R-a)\bar{r}_i + a + R]}\frac{2}{(R-a)}\sum_{n=0}^{N} a_n \left.\frac{d\phi_n}{d\bar{r}}\right|_{\bar{r}=\bar{r}_i} \\ = \frac{K^2}{2}\exp\left(\sum_{n=0}^{N} a_n \phi_n(\bar{r}_i)\right) \\ \left(\frac{2}{(R-a)}\right)^2 \sum_{n=0}^{N} a_n \left.\frac{d^2\phi_n}{d\bar{r}^2}\right|_{\bar{r}=\bar{r}_{N-1}} + \frac{2}{[(R-a)\bar{r}_{N-1} + a + R]}\frac{2}{(R-a)}\sum_{n=0}^{N} a_n \left.\frac{d\phi_n}{d\bar{r}}\right|_{\bar{r}=\bar{r}_{N-1}} \\ = \frac{K^2}{2}\exp\left(\sum_{n=0}^{N} a_n \phi_n(\bar{r}_{N-1})\right) \\ \frac{2}{(R-a)}\sum_{n=0}^{N} a_n \left.\frac{d\phi_n}{d\bar{r}}\right|_{\bar{r}=1} = 0 \end{cases}. \tag{23}$$

This set of equations can be presented in the matrix form. First, the matrix of the derivative of the Chebyshev functions is defined as follows.

$$\frac{d}{dx}\begin{bmatrix} T_0(x) \\ T_1(x) \\ T_2(x) \\ \vdots \\ T_{N-1}(x) \end{bmatrix}_{N\times 1} = \mathbf{D_T}\begin{bmatrix} T_0(x) \\ T_1(x) \\ T_2(x) \\ \vdots \\ T_{N-1}(x) \end{bmatrix}_{N\times 1}, \qquad \mathbf{T} \equiv \begin{bmatrix} T_0(x) \\ T_1(x) \\ T_2(x) \\ \vdots \\ T_{N-1}(x) \end{bmatrix}_{N\times 1}$$
$$\Rightarrow \frac{d^n}{dx^n}\mathbf{T} = \mathbf{D}_\mathbf{T}^n\mathbf{T}. \tag{24}$$

if N is odd, then the matrix denoted by $\mathbf{D_T}$ is reduced to

$$\mathbf{D_T} = \begin{bmatrix} 0 & 0 & 0 & 0 & 0 & \cdots & 0 \\ 1 & 0 & 0 & 0 & 0 & \cdots & 0 \\ 0 & 4 & 0 & 0 & 0 & \cdots & 0 \\ 3 & 0 & 6 & 0 & 0 & \cdots & 0 \\ 0 & 8 & 0 & 8 & 0 & \cdots & 0 \\ \vdots & \vdots & \vdots & \vdots & \vdots & \ddots & \vdots \\ 0 & 2N-2 & 0 & 2N-2 & 0 & \cdots & 0 \end{bmatrix}_{N\times N}, \tag{25}$$

whereas, if N is even, the following matrix is obtained

$$\mathbf{D_T} = \begin{bmatrix} 0 & 0 & 0 & 0 & 0 & \cdots & 0 \\ 1 & 0 & 0 & 0 & 0 & \cdots & 0 \\ 0 & 4 & 0 & 0 & 0 & \cdots & 0 \\ 3 & 0 & 6 & 0 & 0 & \cdots & 0 \\ 0 & 8 & 0 & 8 & 0 & \cdots & 0 \\ \vdots & \vdots & \vdots & \vdots & \vdots & \ddots & \vdots \\ N-1 & 0 & 2N-2 & 0 & 2N-2 & \cdots & 0 \end{bmatrix}_{N\times N}. \tag{26}$$

Moreover, the matrix of the derivative of the Legendre polynomials is explained as follows.

$$\frac{d}{dx}\begin{bmatrix} P_0(x) \\ P_1(x) \\ P_2(x) \\ \vdots \\ P_{N-1}(x) \end{bmatrix}_{N\times 1} = \mathbf{D_P}\begin{bmatrix} P_0(x) \\ P_1(x) \\ P_2(x) \\ \vdots \\ P_{N-1}(x) \end{bmatrix}_{N\times 1}, \qquad \mathbf{P} \equiv \begin{bmatrix} P_0(x) \\ P_1(x) \\ P_2(x) \\ \vdots \\ P_{N-1}(x) \end{bmatrix}_{N\times 1}$$
$$\Rightarrow \frac{d^n}{dx^n}\mathbf{P} = \mathbf{D}_\mathbf{P}^n\mathbf{P}. \tag{27}$$

where the matrix $\mathbf{D_P}$ for odd and even integers of N is shown below

$$\mathbf{D_P} = \begin{bmatrix} 0 & 0 & 0 & 0 & \cdots & 0 & 0 \\ 1 & 0 & 0 & 0 & \cdots & 0 & 0 \\ 0 & 3 & 0 & 0 & \cdots & 0 & 0 \\ 1 & 0 & 5 & 0 & \cdots & 0 & 0 \\ 0 & 3 & 0 & 7 & \cdots & 0 & 0 \\ \vdots & \vdots & \vdots & \vdots & \ddots & \vdots & \vdots \\ 0 & 3 & 0 & 7 & \cdots & 2N-3 & 0 \end{bmatrix}_{N\times N}, \quad (N = \text{odd}) \tag{28}$$

$$\mathbf{D_P} = \begin{bmatrix} 0 & 0 & 0 & 0 & \cdots & 0 & 0 \\ 1 & 0 & 0 & 0 & \cdots & 0 & 0 \\ 0 & 3 & 0 & 0 & \cdots & 0 & 0 \\ 1 & 0 & 5 & 0 & \cdots & 0 & 0 \\ 0 & 3 & 0 & 7 & \cdots & 0 & 0 \\ \vdots & \vdots & \vdots & \vdots & \ddots & \vdots & \vdots \\ 1 & 0 & 5 & 0 & \cdots & 2N-3 & 0 \end{bmatrix}_{N\times N}, \quad (N = \text{even}). \tag{29}$$

With due attention to these relations, the derivative of the Chebyshev functions as well as the Legendre polynomials with respect to r is equal to:

$$\frac{d}{dr}\mathbf{T}(\bar{r}) = \frac{d\bar{r}}{dr}\frac{d}{d\bar{r}}\mathbf{T}(\bar{r}) = \frac{2}{(R-a)}\mathbf{D_T}\mathbf{T}(\bar{r}), \frac{d}{dr}\mathbf{P}(\bar{r}) = \frac{d\bar{r}}{dr}\frac{d}{d\bar{r}}\mathbf{P}(\bar{r}) = \frac{2}{(R-a)}\mathbf{D_P}\mathbf{P}(\bar{r}). \tag{30}$$

Based upon these matrices, the set of the equations, namely Eq. (23), is presented below for the Chebyshev functions in matrix form.

$$\mathbf{L_T^t A} = \mathbf{B_T}, \mathbf{L_T} = \left(\frac{2}{(R-a)}\right)^2 \mathbf{D_T^2}[0 \quad \mathbf{T}(\bar{r}_1) \quad \cdots \quad \mathbf{T}(\bar{r}_i) \quad \cdots \quad \mathbf{T}(\bar{r}_{N-1}) \quad 0]_{(N+1)\times(N+1)} + \frac{2}{(R-a)}\mathbf{D_T}\left[\mathbf{T}(-1) \quad \frac{2}{[(R-a)\bar{r}_1+a+R]}\mathbf{T}(\bar{r}_1) \quad \cdots \quad \frac{2}{[(R-a)\bar{r}_i+a+R]}\mathbf{T}(\bar{r}_i) \quad \cdots \quad \frac{2}{[(R-a)\bar{r}_{N-1}+a+R]}\mathbf{T}(\bar{r}_{N-1}) \quad \mathbf{T}(1)\right]_{(N+1)\times(N+1)}, \tag{31}$$

where

$$, \mathbf{A} = \begin{bmatrix} a_0 \\ a_1 \\ \vdots \\ a_i \\ \vdots \\ a_{N-1} \\ a_N \end{bmatrix}_{(N+1)\times 1}, \quad \mathbf{B_T} = \begin{bmatrix} -\frac{2}{\xi}a \\ \frac{K^2}{2}\exp\left(\sum_{n=o}^{N} a_n T_n(\bar{r}_1)\right) \\ \vdots \\ \frac{K^2}{2}\exp\left(\sum_{n=o}^{N} a_n T_n(\bar{r}_i)\right) \\ \vdots \\ \frac{K^2}{2}\exp\left(\sum_{n=o}^{N} a_n T_n(\bar{r}_{N1})\right) \\ 0 \end{bmatrix}_{(N+1)\times 1}. \tag{32}$$

Moreover, one may obtain the set of Eq. (23) for the Legendre polynomials in the following matrix form.

$$\mathbf{L_P^t A} = \mathbf{B_P}, \mathbf{L_P} = \left(\frac{2}{(R-a)}\right)^2 \mathbf{D_P^2}[0 \quad \mathbf{P}(\bar{r}_1) \quad \cdots \quad \mathbf{P}(\bar{r}_i) \quad \cdots \quad \mathbf{P}(\bar{r}_{N-1}) \quad 0]_{(N+1)\times(N+1)} + \frac{2}{(R-a)}\mathbf{D_P}\left[\mathbf{P}(-1) \quad \frac{2}{[(R-a)\bar{r}_1+a+R]}\mathbf{P}(\bar{r}_1) \quad \cdots \quad \frac{2}{[(R-a)\bar{r}_i+a+R]}\mathbf{P}(\bar{r}_i) \quad \cdots \quad \frac{2}{[(R-a)\bar{r}_{N-1}+a+R]}\mathbf{P}(\bar{r}_{N-1}) \quad \mathbf{P}(1)\right]_{(N+1)\times(N+1)}, \tag{33}$$

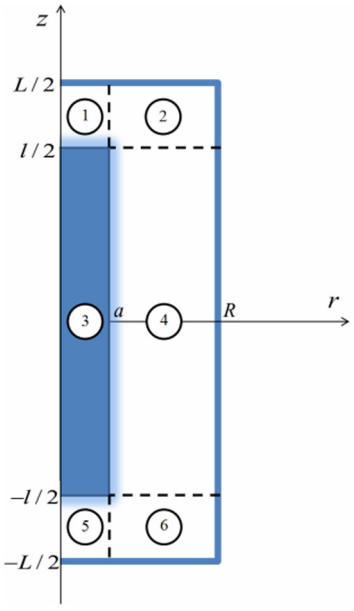

Fig. 1. The domain is divided into six sub-domains, which is the minimum division to use the pseudo-spectral method. The sub-domain that is numbered "3" corresponds to the region inside the macromolecule.

where the matrices $\mathbf{A}$ and $\mathbf{B_P}$ are defined below

$$\mathbf{A} = \begin{bmatrix} a_0 \\ a_1 \\ \vdots \\ a_i \\ \vdots \\ a_{N-1} \\ a_N \end{bmatrix}_{(N+1)\times 1}, \mathbf{B_P} = \begin{bmatrix} -\frac{2}{\xi}a \\ \frac{K^2}{2}\exp\left(\sum_{n=o}^{N} a_n \mathbf{P}_n(\bar{r}_1)\right) \\ \vdots \\ \frac{K^2}{2}\exp\left(\sum_{n=o}^{N} a_n \mathbf{P}_n(\bar{r}_i)\right) \\ \vdots \\ \frac{K^2}{2}\exp\left(\sum_{n=o}^{N} a_n \mathbf{P}_n(\bar{r}_{N1})\right) \\ 0 \end{bmatrix}_{(N+1)\times 1}. \tag{34}$$

In what follows, the mathematical formulation of the pseudo-spectral method is discussed for a two-dimensional equation.

The pseudo-spectral method can be applied for solving PDEs on an arbitrary computational domain. To have an accurate pseudo-spectral method, we should divide the computational domain into some sub-domains. Also, on each sub-domain, the corresponding physical equation must be defined. Furthermore, each sub-domain must be converted to reference sub-domain, namely $\Omega_s = [-1,1] \times [-1,1]$, for distributing the used collocation points in pseudo-spectral method. Using more sub-domains enables us to overcome the round-off error in computer system.

Therefore, in order to apply the pseudo-spectral technique, the domain is divided into six sub-domains with minimum divisions, which is depicted in Fig. 1. To obtain an approximate solution of Eq. (1) the following polynomial form is used.

$$\begin{cases} \left(\frac{\partial^2}{\partial r^2}+\frac{1}{r}\frac{\partial}{\partial r}+\frac{\partial^2}{\partial z^2}\right)y(r,z)=\frac{K^2}{2}e^{y}, \quad y(r,z)\simeq \bar{u}_i(\bar{r},\bar{z}), i=1,2,4,5,6 \\ \left(\frac{\partial^2}{\partial r^2}+\frac{1}{r}\frac{\partial}{\partial r}+\frac{\partial^2}{\partial z^2}\right)y(r,z)=0, \quad y(r,z)\simeq \bar{u}_3(\bar{r},\bar{z}) \end{cases} \text{and}$$

$$\bar{u}_i(\bar{r},\bar{z})=\sum_{n=0}^{N}\sum_{m=0}^{M}a_{nm}^{i}\phi_n(\bar{r})\phi_m(\bar{z}), \quad i=1,2,3,4,5,6 \tag{35}$$

where $\bar{u}_3(\bar{r},\bar{z})$ corresponds to the region inside the macromolecule. As the arguments $\bar{r}$ and $\bar{z}$ are considered in interval $[-1, 1]$, the corresponding intervals for r and z, namely $[a, b]$ and $[c, d]$, can be reproduced as follows

$$r=\frac{1}{2}[(b-a)\bar{r}+a+b], \tag{36}$$

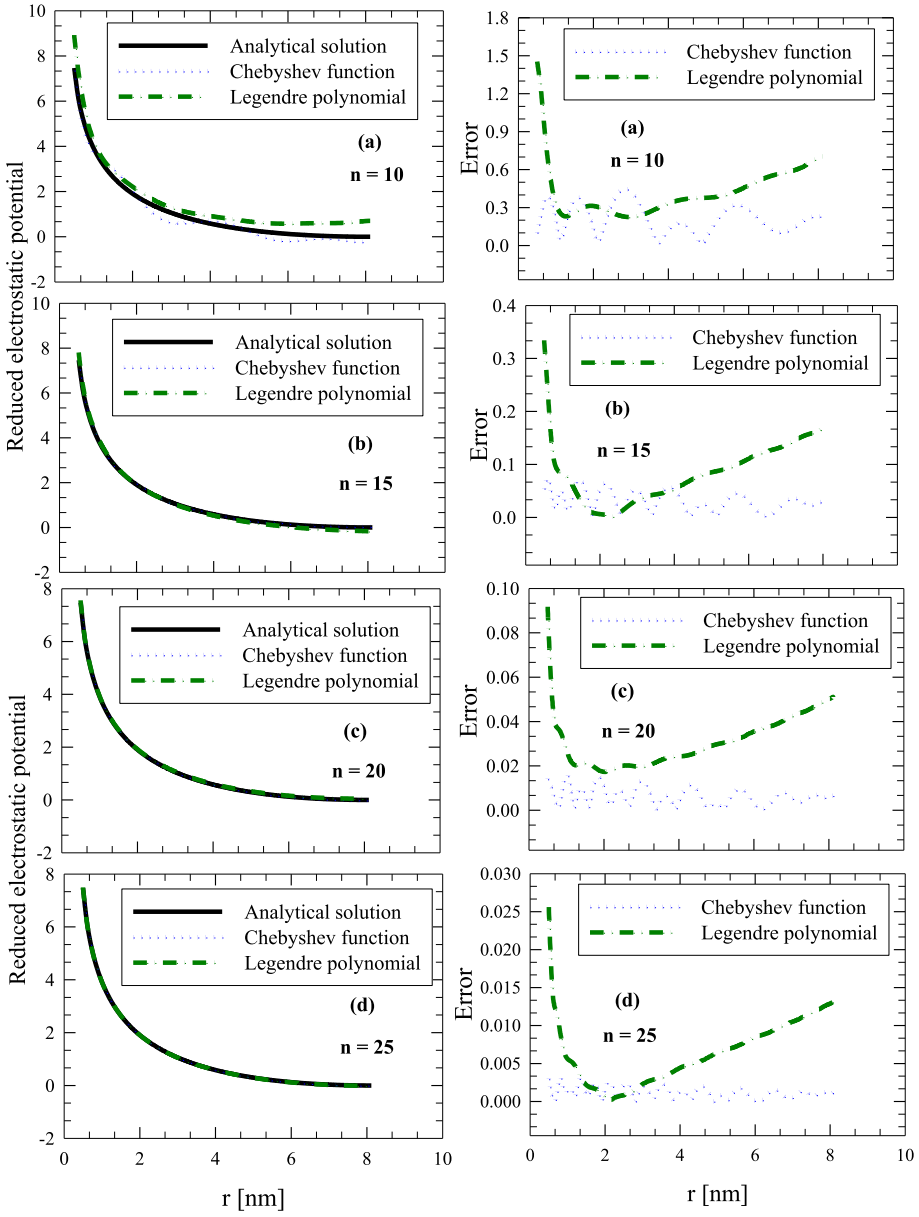

Fig. 2. The dimensionless reduced electric potential obtained from the analytical solution, i.e. Eq. (11) in comparison with our numerical method for a long macromolecule as well as the associated error. The orthogonal functions used in our method are the Legendre polynomials and Chebyshev functions for various number of points: (a) $n = 10$, (b) $n = 15$, (c) $n = 20$ and (d) $n = 25$.

$$z = \frac{1}{2}[(d-c)\bar{z} + c + d]. \tag{37}$$

The intervals $[a, b]$ and $[c, d]$ are determined in each sub-domain as illustrated in Fig. 1. In Eq. (35), a_{nm} for $n = 0,\ldots, N$ and $m = 0,\ldots, M$ are the coefficients should be obtained. Moreover, $\phi_n(\bar{r})$ and $\phi_m(\bar{z})$ are the orthogonal functions, which either the Legendre polynomials or the Chebyshev functions can be considered with the arguments $\bar{r}$ and $\bar{z}$ lying in the interval $[-1, 1]$. Eq. (35) is subjected to the following boundary condition for the macromolecule stated in this study

$$\mathbf{n} \cdot (\mathbf{D}_{\text{inside}} - \mathbf{D}_{\text{outside}}) = \sigma, \tag{38}$$

where $\mathbf{n}$ is normal unit vector to the surface from outside to inside of the macromolecule. Furthermore, $\sigma = \frac{e}{2\pi ab}$ stands for the surface charge density of the macromolecule [28]. Besides, $\mathbf{D}_{\text{inside}}$ and $\mathbf{D}_{\text{outside}}$ denote the electric displacement vectors for the inside and outside of the macromolecule, respectively. Therefore, the Neumann boundary conditions on the macromolecule can be written in the following form

$$\begin{cases} \varepsilon_3 \frac{d\bar{u}_3(\bar{r},\bar{z})}{dr}|_{r=a,-\frac{l}{2}\leqslant z\leqslant\frac{l}{2}} - \varepsilon_4 \frac{d\bar{u}_4(\bar{r},\bar{z})}{dr}|_{r=a,-\frac{l}{2}\leqslant z\leqslant\frac{l}{2}} = \frac{e\sigma}{k_B T}, \\ \varepsilon_3 \frac{d\bar{u}_3(\bar{r},\bar{z})}{dz}|_{r\leqslant a,z=\frac{l}{2}} - \varepsilon_1 \frac{d\bar{u}_1(\bar{r},\bar{z})}{dz}|_{r\leqslant a,z=\frac{l}{2}} = \frac{e\sigma}{k_B T}, \\ \varepsilon_3 \frac{d\bar{u}_3(\bar{r},\bar{z})}{dz}|_{r\leqslant a,z=-\frac{l}{2}} - \varepsilon_5 \frac{d\bar{u}_5(\bar{r},\bar{z})}{dz}|_{r\leqslant a,z=-\frac{l}{2}} = \frac{e\sigma}{k_B T}. \end{cases} \tag{39}$$

The dielectric constant of the macromolecule is usually taken to be approximately 3 [31]. For the boundaries with no surface charge density, Eq. (38) yields

$$\begin{cases} \frac{d\bar{u}_2(\bar{r},\bar{z})}{dr}|_{r=a,z>\frac{l}{2}} = \frac{d\bar{u}_1(\bar{r},\bar{z})}{dr}|_{r=a,z>\frac{l}{2}}, \\ \frac{d\bar{u}_2(\bar{r},\bar{z})}{dz}|_{r>a,z=\frac{l}{2}} = \frac{d\bar{u}_4(\bar{r},\bar{z})}{dz}|_{r>a,z=\frac{l}{2}}, \\ \frac{d\bar{u}_6(\bar{r},\bar{z})}{dr}|_{r=a,z<-\frac{l}{2}} = \frac{d\bar{u}_5(\bar{r},\bar{z})}{dr}|_{r=a,z<-\frac{l}{2}}, \\ \frac{d\bar{u}_6(\bar{r},\bar{z})}{dz}|_{r>a,z=-\frac{l}{2}} = \frac{d\bar{u}_4(\bar{r},\bar{z})}{dz}|_{r>a,z=-\frac{l}{2}}. \end{cases} \tag{40}$$

The continuity condition for the electric potential gives

$$\begin{cases} \bar{u}_3(\bar{r},\bar{z})|_{r=a,-\frac{l}{2}\leqslant z\leqslant\frac{l}{2}} = \bar{u}_4(\bar{r},\bar{z})|_{r=a,-\frac{l}{2}\leqslant z\leqslant\frac{l}{2}}, \\ \bar{u}_3(\bar{r},\bar{z})|_{r\leqslant a,z=\frac{l}{2}} = \bar{u}_1(\bar{r},\bar{z})|_{r\leqslant a,z=\frac{l}{2}}, \\ \bar{u}_3(\bar{r},\bar{z})|_{r\leqslant a,z=-\frac{l}{2}} = \bar{u}_5(\bar{r},\bar{z})|_{r\leqslant a,z=-\frac{l}{2}} \end{cases} \tag{41}$$

It is notable that by considering the same boundary condition for each sub-domain in common boundaries, i.e. the boundaries with no surface charge, the same number of equations appears in the set of equations. As a conclusion, the set of equations cannot be solved. Therefore, it is necessary that for each common boundary the Dirichlet boundary condition is attributed to a sub-domain and the Neumann boundary condition is attributed to another sub-domain. For this purpose, the Dirichlet boundary conditions are mentioned in addition to the Neumann boundary conditions, i.e. Eq. (40).

$$\begin{cases} \bar{u}_2(\bar{r},\bar{z})|_{r=a,z>\frac{l}{2}} = \bar{u}_1(\bar{r},\bar{z})|_{r=a,z>\frac{l}{2}}, \\ \bar{u}_2(\bar{r},\bar{z})|_{r>a,z=\frac{l}{2}} = \bar{u}_4(\bar{r},\bar{z})|_{r>a,z=\frac{l}{2}}, \\ \bar{u}_6(\bar{r},\bar{z})|_{r=a,z<-\frac{l}{2}} = \bar{u}_5(\bar{r},\bar{z})|_{r=a,z<-\frac{l}{2}}, \\ \bar{u}_6(\bar{r},\bar{z})|_{r>a,z=-\frac{l}{2}} = \bar{u}_4(\bar{r},\bar{z})|_{r>a,z=-\frac{l}{2}}. \end{cases} \tag{42}$$

With due attention to the electroneutrality of the system, the Neumann boundary condition for the unit cell is shown below.

$$\begin{cases} \frac{d\bar{u}_i(\bar{r},\bar{z})}{dr}|_{r=R} = 0, & i = 2,4,6 \\ \frac{d\bar{u}_j(\bar{r},\bar{z})}{dz}|_{z=\frac{l}{2}} = 0, & j = 1,2 \\ \frac{d\bar{u}_j(\bar{r},\bar{z})}{dz}|_{z=-\frac{l}{2}} = 0. & j = 5,6 \end{cases} \tag{43}$$

The partial differential Eq. (35) with the boundary conditions defined by Eqs. (38)–(43) should be solved. These form a set of nonlinear equations. We did not present the matrix forms due to the complexity of this set of equations.

Numerical results and discussion

One can see from Fig. 2 that the dimensionless reduced electric potential, which is obtained from the analytical solution, i.e. Eq. (11), is compared with our numerical method for one-dimensional PBE corresponding to a long macromolecule. It is notable that, in our method, orthogonal functions such as the Legendre polynomials and Chebyshev functions based on the various numbers of points are used. Afterwards, the error of the presented method is computed.

As a conclusion, the accuracy of the Chebyshev functions with specified number of collocation points (Chebyshev-Gauss) is more than that of the Legendre polynomials with the same number of points (Legendre-Gauss-Lobatto). This is an expected result because the interpolation using the Chebyshev nodes has minimum error based on an infinity norm [15,32]. Besides, it is concluded that by considering merely 25 collocation points, one may approach the exact solution, which satisfies the enough accuracy in our numerical method.

In Fig. 3, validations for the two-dimensional PBE are performed for the two extreme cases of infinite length and large plate, which

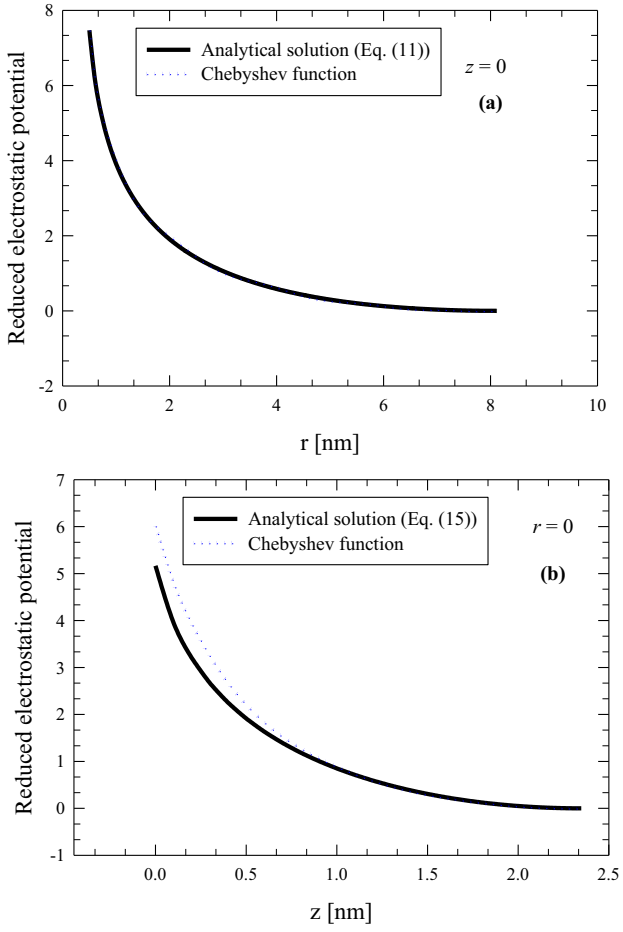

Fig. 3. Comparison of the solutions obtained for the two-dimensional PBE based on the Chebyshev function, considering $n = 15$ for each sub-domain for r and z, associated with the analytical solutions in two extreme cases: (a) the infinite length and (b) the large plate.

are properly explained by a one-dimensional PBE. The analytical solutions corresponding to the cases are shown from Eqs. (11) and (15), respectively. It is worth mentioning that, the results obtained from the pseudo-spectral method merely on the basis of the Chebyshev functions are plotted in Fig. 3 due to the higher accuracy in comparison with the Legendre polynomials. As shown in the figure, satisfactory agreements are found between the analytical and numerical solutions.

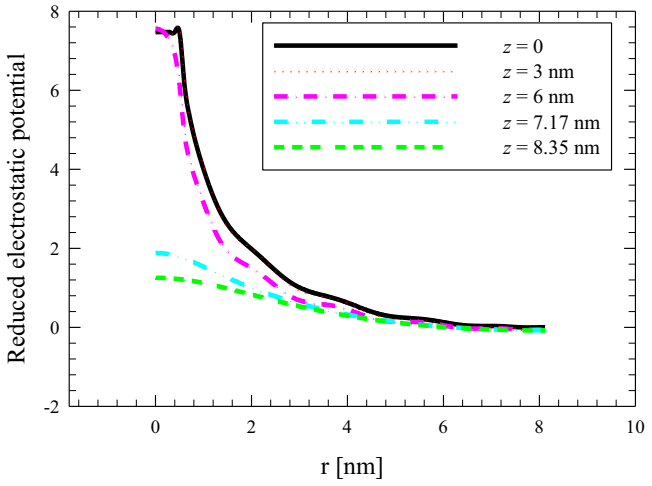

Fig. 4. Reduced electric potential obtained from the two-dimensional PBE as a function of r for various values of z.

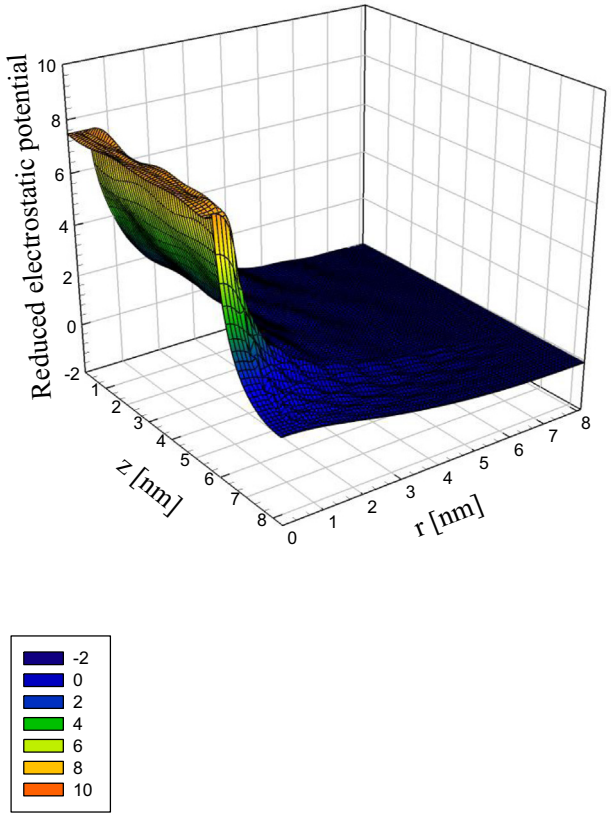

Fig. 5. Three-dimensional graph of the reduced electric potential obtained from the two-dimensional PBE.

The solution of the two-dimensional PBE as a function of r and for various values of z is illustrated in Fig. 4. It should be noted that in the analysis, the values for the radius and height of the unit cell are considered to be as 8.1 and 16.7 nm, respectively. In addition, for more clarification, the solution of the two-dimensional PBE in three dimensions is plotted in Fig. 5.

Conclusion

The height and radius of the unit cell were properly obtained to be as 16.7 nm and 8.1 nm, respectively, considering the macromolecule concentration as well as the corresponding electric fields. Afterwards, for a rodlike macromolecule in the salt free solution, the electric potential was computed by solving a two-dimensional PBE based upon the pseudo-spectral method. Besides, for the two special cases, comparisons were made between our numerical results and the analytical solutions for one-dimensional PBE, and good agreements were found. We drew a conclusion that, for the same number of points, the method based on the Chebyshev functions is more accurate as compared to the method based upon the Legendre polynomials. Moreover, it was concluded that by considering 25 collocation points for r and z, the exact enough solution can be obtained, which demonstrates efficiency of our numerical method. It is notable that numerical solution of the PBE for a rodlike macromolecule has not been reported in the literature previously using the pseudo-spectral method.

Appendix A. Supplementary data

Supplementary data associated with this article can be found, in the online version, at https://doi.org/10.1016/j.rinp.2017.10.024.

References

[1] Holm C, Kekicheff P, Podgornik R. Electrostatic Effects in Soft Matter and Biophysics. Dordrecht: Kluwer Academic; 2001.
[2] Poon WCK, Andelman D. Soft Condensed Matter Physics in Molecular and Cell Biology. New York: Taylor & Francis; 2006.
[3] Oosawa F. Polyelectrolytes. New York: Marcel Dekker; 1971.
[4] Zhao-Yang T, Yue-Jin Z, Chao-Hui T. Self-consistent field theory of adsorption of flexible polyelectrolytes onto an oppositely charged sphere. Chin Phys B 2014;23:038202–38206.
[5] French RH et al. Long range interactions in nanoscale science. Rev Mod Phys 2010;82:1887–944.
[6] Honig B, Nicholls A. Classical electrostatics in biology and chemistry. Science 1995;268:1144–9.
[7] Rocchia W, Alexov E, Honig B. Extending the applicability of the nonlinear Poisson–Boltzmann equation: multiple dielectric constants and multivalent ions. J Phys Chem B 2001;105:6507–14.
[8] Khan M, Farooq A, Azeem Khan W, Hussain M. Exact solution of an electroosmotic flow for generalized Burgers fluid in cylindrical domain. Results Phys 2016;6:933–9.
[9] Yang QN, Zheng JJ, Miao Y, Sima YZ. An improved hybrid boundary node method for solving steady fluid flow problems. Eng Anal Bound Elem 2011;35:18–24.
[10] Morton KW, Mayers DF. Numerical Solution of Partial Differential Equations. Cambridge: Cambridge University Press; 2005.
[11] Alonso N, Bowers KL. An alternating-direction sinc-galerkin method for elliptic problems. J Complexity 2009;25:237–52.
[12] Fairweather G, Karageorghis A, Maack J. Compact optimal quadratic spline collocation methods for the Helmholtz equation. J Comput Phys 2011;230:2880–95.
[13] Liu N, Lin EB. Legendre wavelet method for numerical solutions of partial differential equations. Numer Methods Partial Differ Equation 2010;26:81–94.
[14] Davari A, Ahmadi A. New implementation of Legendre polynomials for solving partial differential equations. Appl Math 2013;4:1647–50.
[15] Hesthaven JS, Gottlieb S, Gottlieb D. Spectral Methods for Time-Dependent Problems. Cambridge: Cambridge University Press; 2007.
[16] Shen J, Tang T, Wang T. Spectral methods, Algorithms, Analysis and Applications. New York: Springer-Verlag Berlin Heidelberg; 2011.
[17] Boyd JP. Chebyshev and Fourier Spectral Methods. 2nd ed. New York: Dover Publications; 1999.

[18] Canuto C, Hussaini MY, Quarteroni A, Zang TA. Spectral Methods, Evolution to Complex Geometries and Applications to Fluid Dynamics. New York: Springer-Verlag Berlin Heidelberg; 2007.
[19] Güner A, Yalçınbaş S. Legendre Collocation method for solving nonlinear Differential equations. Math Comput Appl 2013;18:521–30.
[20] Li Z-C, Lu T-T, Hu H-Y, Cheng AH-D. Trefftz and Collocation Methods. Boston: WIT Press; 2008.
[21] Deshkovski A, Obukhov S, Rubinstein M. Counter ion phase transitions in dilute polyelectrolyte solutions. Phys Rev Lett 2001;86:2341–4.
[22] Steinmoeller DT, Stastna M, Lamb KG. Pseudospectral methods for Boussinesq-type equations in an annular domain with applications to mid-sized lakes. J Comput Sci 2013;4:3–11.
[23] Shamsi M, Dehghan M. Determination of a control function in three-dimensional parabolic equations by Legendre pseudospectral method. Numer Methods Partial Differ Equation 2010. https://doi.org/10.1002/num.20608.
[24] Khaksar-e Oshagh M, Shamsi M. Direct pseudo-spectral method for optimal control of obstacle problem–an optimal control problem governed by elliptic variational inequality. Math Meth Appl Sci 2017. https://doi.org/10.1002/mma.4366.
[25] Nikzad S, Noshad H, Saviz M. Steady state behavior of a finite rodlike macromolecule in salt free solution. Results Phys 2017;7:2658–62.
[26] Alfrey T, Berg P, Morawetz H. The counter ion distribution in solutions of rod-shaped polyelectrolytes. J Polym Sci 1951;7:543–7.
[27] Yoshida M, Kikuchi K, Maekawa T, Watanabe H. Electric polarization of rodlike Polyions investigated by Monte Carlo simulations. J Phys Chem 1992;96:2365–71.
[28] LeBret M, Zimm BH. Distribution of counter ions around a cylindrical polyelectrolyte and manning's condensation theory. Biopolymers 1984;23:287–312.
[29] Fuoss R, Katchalsky A, Lifson S. The potential of an infinite rod-like molecule and the distribution of the counter ions. Proc Natl Acad Sci U S A 1951;37:579–89.
[30] Deserno M, Holm C, May S. The fraction of condensed counter ions around a charged rod: Comparison of Poisson-Boltzmann theory and computer simulations. Macromolecules 2000;33:199–206.
[31] Grant EH. The dielectric method of investigating bound water in biological material: an appraisal of the technique. Bioelectromagnetics 1982;3:17–24.
[32] Burden RL, Faires JD. Numerical Analysis. 9th ed. Boston: Richard Stratton; 2004.